Resonant optical alignment and orientation of Mn^{2+} spins in CdMnTe crystals

K. A. Baryshnikov,[1,*] L. Langer,[2] I. A. Akimov,[1,2] V. L. Korenev,[1] Yu. G. Kusrayev,[1] N. S. Averkiev,[1] D. R. Yakovlev,[1,2] and M. Bayer[1,2]

[1]*Ioffe Institute, Russian Academy of Sciences, 194021 St. Petersburg, Russia*

[2]*Experimentelle Physik 2, Technische Universität Dortmund, 44221 Dortmund, Germany*

(Received 14 July 2015; revised manuscript received 10 October 2015; published 11 November 2015)

We report on spin orientation and alignment of Mn^{2+} ions in (Cd,Mn)Te diluted magnetic semiconductor crystals using resonant intracenter excitation with circular- and linear-polarized light. The resulting polarized emission of the magnetic ions is observed at low temperatures when the spin relaxation time of the Mn^{2+} ions is in the order of 1 ms, which considerably exceeds the photoluminescence decay time of 23 μs. We demonstrate that the experimental data on optical orientation and alignment of Mn^{2+} ions can be explained using a phenomenological model that is based on the approximation of isolated centers.

DOI: 10.1103/PhysRevB.92.205202 PACS number(s): 78.30.Fs, 75.50.Pp, 78.47.D−

I. INTRODUCTION

Optically addressed defects in semiconductors have great potential for applications in the field of quantum information and sensing techniques [1]. First, an isolated defect possesses long optical and spin coherence times. Second, control of charge and spin states by resonant optical excitation may be used as a tool for ultrafast switching of quantum-mechanical states. Current activities on optical control of spin states in defects have been mainly focused on diamond (nitrogen-vacancy center) [2,3] and silicon carbide [4–7]. These efforts allowed one to demonstrate resonant optical pumping and local detection of tiny magnetic fields [8,9]. However, there are also some drawbacks like in the case of diamond, the fabrication of high purity structures representing an expensive and challenging task. It is therefore important and desirable to extend such studies to semiconductor materials with high mobility of carriers, e.g., GaAs, Si, and CdTe. This would allow one to use electrical currents for spin and charge control of optically addressed centers.

Manganese atoms ($3d^5 4s^2$) in II-VI semiconductors form Mn^{2+} isovalent centers which substitute the cadmium atoms in a CdTe crystal [10,11]. It is possible to introduce Mn atoms in a wide concentration range up to 100%. This is the basis of the class of materials called diluted magnetic semiconductors [12]. The Mn^{2+} ion has five electrons on the outer $3d$ shell. Due to the strong electron-electron interaction the system is a high-spin complex in a weak crystal field. The ground state is a spin sextet $^6A_1$, which corresponds to total spin $S = 5/2$.

There is only one orbital state of the system that corresponds to total angular momentum $L = 0$ according to the Pauli principle [10,11]. It is possible to excite the Mn^{2+} ion using the direct optical transition to the $^4T_1$ state with nonzero orbital momentum and $S = 3/2$ [10,11]. Alternatively, the Mn^{2+} ion can be excited via energy transfer from optically excited electron-hole pairs and excitons [13,14]. The relaxation into the ground state is accompanied by photon emission, i.e., intracenter photoluminescence (PL), with photon energies around 2.0 eV occurring during characteristic decay times of about several tens of microseconds [15,16]. Thus, the Mn^{2+} ion is an optically active center in the red-yellow spectral range and it can be considered as a good candidate for optical control of spin by polarized light. Spin transfer from optically oriented electron-hole pairs to single Mn^{2+} ion in the ground state via strong exchange interaction was recently demonstrated in CdTe quantum dots [17,18]. However, up to now resonant optical orientation and alignment of Mn^{2+} spins in diluted magnetic semiconductors has not been realized.

In this paper we report on optical orientation and optical alignment of Mn^{2+} ions in their excited states using resonant excitation with circular- and linear-polarized light, respectively, in (Cd,Mn)Te crystals with Mn concentrations of about 40%. Time- and polarization-resolved PL measurements show that the characteristic relaxation times for circular and linear polarization of the intracenter PL exceed 1 ms, which are significantly longer than the PL decay time. The largest values of PL polarization are obtained at low temperatures when the Mn spin relaxation is suppressed. A transparent theoretical model addressing optical alignment and optical orientation of a single Mn^{2+} ion under resonant optical excitation allows us to explain the observed values of PL polarization.

II. EXPERIMENT

The investigated samples were prepared from an ingot of bulk $Cd_{1-x}Mn_xTe$ grown by the Bridgman technique. The crystals were cut along the (110) cleavage plane and had sizes of about $5\times5\times0.5$ mm^3. Structures with different Mn content x varying from 0.36 to 0.45 were studied. The samples were mounted in a He-bath cryostat with a variable temperature inset and the measurements were performed at temperature $T = 8$ K. For nonresonant excitation we used a continuous-wave blue-emitting laser diode with photon energy $\hbar\omega_{exc} = 3.06$ eV. Resonant excitation of Mn^{2+} ions was accomplished by a tunable optical parametric oscillator which was synchronously pumped with a Kerr-lens mode-locked Ti:sapphire laser. The emitted optical pulses had a duration of 2–3 ps and a spectral width of about 1 nm, at a repetition rate of 76.75 MHz. For time-resolved measurements we used an electro-optical modulator with a rise time of about 20 ns in the excitation beam path. This allowed us to generate well defined trains of pulses with duration of 5 μs at a repetition rate of 10 kHz. The laser beam was focused

*barysh.1989@gmail.com

into a spot with diameter of about 100 μm and the excitation power density did not exceed 100 W/cm^2. In all measurements the emission signal was dispersed with a single imaging monochromator with linear dispersion of 6.5 nm/mm. Time-integrated spectra were detected with a charge-coupled device, while for time-resolved measurements with electro-optical modulator we used a streak camera. For polarization-resolved measurements a Glan prism in combination with quarter- and half-wave plates were introduced in the excitation and detection paths. The degree of circular polarization was determined as $\rho_c^{\rm exc} = (I_+ - I_-)/(I_+ + I_-)$, where I_+ and I_- are the σ^+ and σ^- polarized PL intensities, respectively. The degree of linear polarization is defined as $\rho_l^{\rm exc} = (I_x - I_y)/(I_x + I_y)$ and $\rho_{l'}^{\rm exc} = (I_{x'} - I_{y'})/(I_{x'} + I_{y'})$, where I_x, I_y, $I_{x'}$, and $I_{y'}$ are the intensities of the signal detected for linear polarization along the x, y, x', and y' axes, respectively. Here, $\mathbf{x} \| [001]$, $\mathbf{y} \| [1\bar{1}0]$, while x' and y' are rotated by 45° with respect to the x and y axes around the z axis. The Stokes parameters of the PL $\rho_c^{\rm exc}$, $\rho_l^{\rm exc}$, and $\rho_{l'}^{\rm exc}$ were measured for circular-polarized (exc $= +, -$) and linear-polarized (exc $= x, y, x', y'$) excitation.

The time-integrated data are summarized in Fig. 1. The PL spectra under nonresonant excitation comprise two characteristic peaks. One of them, centered at photon energy about 2.0 eV, is attributed to the Mn^{2+} intracenter PL [see Fig. 1(a)]. Its position is independent of the Mn concentration. The other peak corresponds to the exciton PL. The peak undergoes a blue shift with increasing x and follows the band gap shift of (Cd,Mn)Te. Although we do not observe the exciton peak in the crystal with $x = 0.45$, the expected position of the exciton resonance at low temperatures is about 2.31 eV [19].

Under resonant excitation with $\hbar\omega_{\rm exc} \sim 2.2$ eV we observe significant circular and linear polarization of the Mn^{2+} emission band which reach values of about 10% and follow the polarization of the exciting laser [see Fig. 1(b)]. PL excitation (PLE) spectra show a step-like behavior at the photon energy of 2.2 eV which corresponds to resonant optical excitation of the first excited Mn state. The large Stokes shift of about 0.2 eV between the PL and PLE spectra of intracenter transitions in Mn is typical for II-VI crystals [11,15,20,21]. The Stokes shift and its role in the relaxation of the center will be discussed below. The PLE spectra and their polarization follow the same dependence in all three samples showing no correlation with the optical generation of excitons. Therefore we conclude that the optically induced polarization of the intracenter PL is due to direct resonant excitation of the Mn^{2+} ions. The optical orientation of the Mn spins along the light propagation direction $\mathbf{z} \| [110]$ is evidenced by the circular polarization $\rho_c^+ = -\rho_c^-$, while the optical alignment of the Mn^{2+} ions in the xy plane is manifested by the linear polarization $\rho_l^x = -\rho_l^y$ ($\rho_{l'}^x = \rho_{l'}^y = 0$). Here, it is essential that the sign of ρ_c and ρ_l changes when the excitation polarization is switched from σ^+ to σ^- and from x to y, respectively. Moreover, the magnitude of optical alignment does not depend on the direction of linear polarization of the excitation, i.e., $\rho_l^x \approx \rho_{l'}^{x'}$, which suggests a weak anisotropy for the observed effect.

Time-resolved PL measurements give insight into the relaxation dynamics after pulsed optical excitation. The total PL intensity $I(t) = I_+ + I_- = I_x + I_y$ follows the population decay $I(t) \propto \exp(-t/\tau)$ and therefore allows us to determine

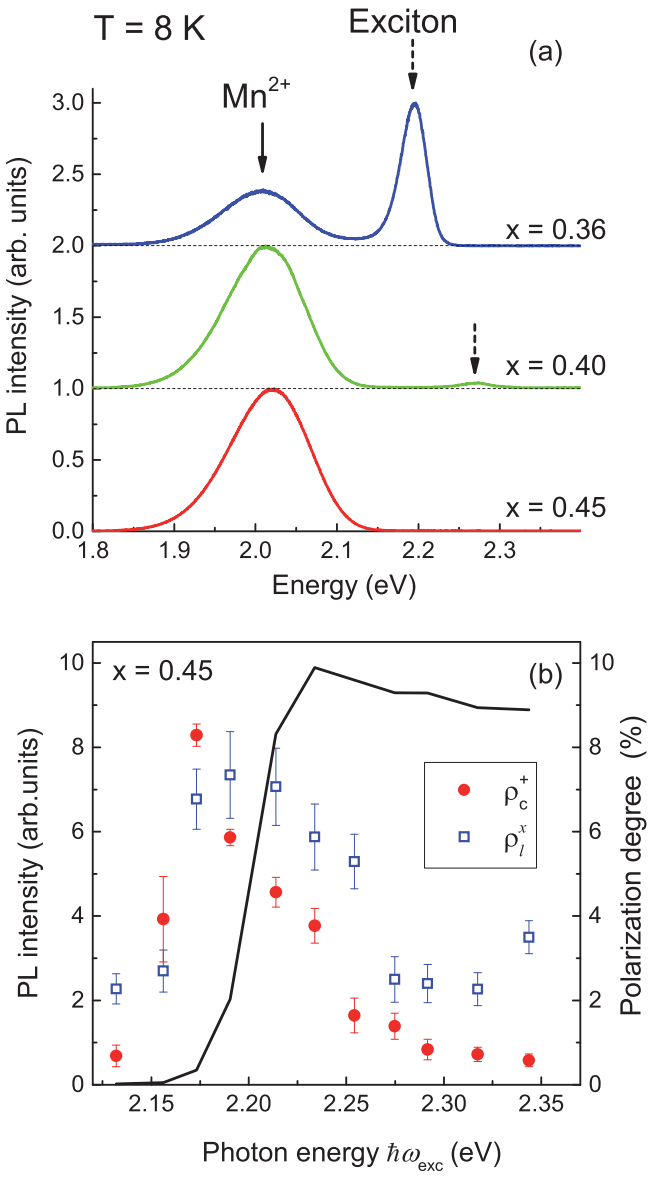

FIG. 1. (Color online) Time-integrated photoluminescence data. (a) PL spectra of three samples with different Mn content x for photon excitation energy $\hbar\omega_{\rm exc} = 3.06$ eV. The solid arrow indicates the intracenter Mn^{2+} PL band at about 2.0 eV. The dashed arrows indicate the exciton PL peak. (b) Dependence of the Mn intracenter PL intensity (solid line), the circular ρ_c^+ (circles), and linear ρ_l^x (squares) polarization degrees as functions of $\hbar\omega_{\rm exc}$ under quasiresonant excitation of the Mn^{2+} ions in $Cd_{0.55}Mn_{0.45}Te$. The excitation is σ^+ and linear along x polarized for ρ_c^+ and ρ_l^x, respectively.

the lifetime τ of the Mn^{2+} excited state. Polarization transients give direct access to the spin dynamics of the optically oriented or aligned spins of the Mn^{2+} ions and allow us to measure the approximate value of the spin relaxation time.

The experimental data measured in the sample with $x = 0.40$ for photon excitation energy $\hbar\omega_{\rm exc} = 2.175$ eV are presented in Fig. 2. From the intensity transient we evaluate the lifetime of 23 μs, which is in good agreement with previous studies [15,16]. It follows from Fig. 2(b) that the spin relaxation is very slow. The circular polarization ρ_c is

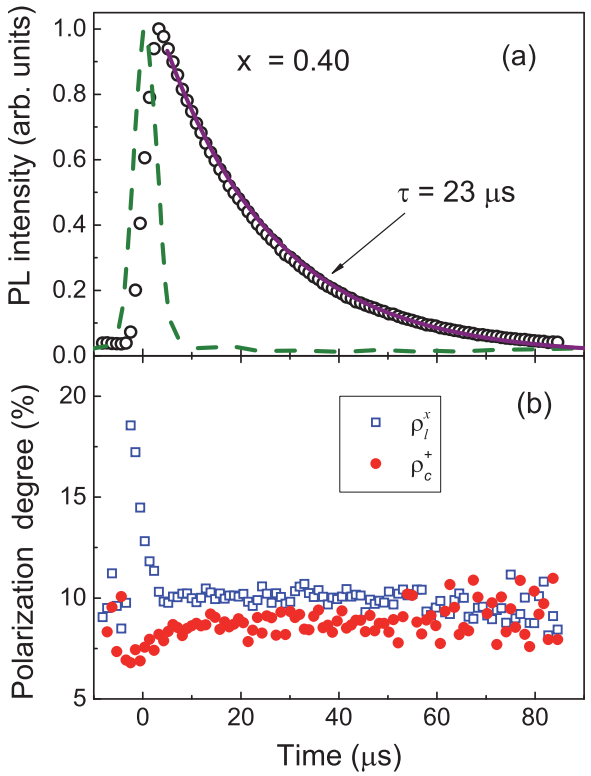

FIG. 2. (Color online) Time-resolved PL data for the $Cd_{0.60}Mn_{0.40}Te$ crystal under excitation at $\hbar\omega_{exc} = 2.175$ eV. Circular-polarized optical pulses each with duration of 5 μs excite the sample every 100 μs. (a) PL intensity transients. The solid line is an exponential fit with decay time $\tau = 23$ μs. The dashed line is the apparatus function of the setup. (b) Circular ρ_c and linear ρ_l polarization dynamics.

constant over the whole range of 80 μs. In the case of linear polarization we observe a fast initial decay, which we cannot resolve, followed by a plateau. Taking into account that the standard deviation of the polarization degree is about 0.1 of the average value we estimate that the decay time has to be at least an order of magnitude longer than the time range of scan ($\sim$100 μs). Therefore we evaluate the spin relaxation time, which is in the order of 1 ms or longer.

III. THEORY AND DISCUSSION

In the following we present a simple theoretical description of optical orientation and optical alignment for the case of isolated Mn^{2+} ions. This model will help us to estimate the theoretical restrictions on the magnitudes of intracentral PL polarization degrees. The ground and excited states of the center represent complex many-particle wave functions. Inner d–d transitions in an isolated Mn^{2+} ion are forbidden by spin and parity selection rules, but they become partly allowed due to different effects, such as the spin-orbit interaction, the presence of noninversion components of the crystal field and considerable hybridization of d states with p states of the chalcogenides [11]. We will not discuss the detailed many-particle structure of the electronic states of the center. Let us consider only the effect of the spin-orbit interaction in the approximation of spherical symmetry. It allows us to build a model of intracenter transitions with selection rules for electric-dipole transitions in one-particle approximation using the total angular momentum formalism.

As was mentioned above, the ground state of Mn^{2+} ion is the sixfold degenerated term $^6A_1$, which corresponds to total spin $S = 5/2$ and total orbital momentum $L = 0$. Therefore we will treat it as a spherically symmetric state with the total angular momentum $j = 5/2$. The first excited state is $^4T_1$ [10,11], which corresponds to total spin $S = 3/2$. Note that the orbital state T_1 can be associated with effective total orbital momentum $L_{eff} = 1$ (as the wave functions of the appropriate irreducible representation transform by rotations of the coordinates like functions of the corresponding orbital momentum). So in the spherical approximation for the spin-orbit interaction we can distinguish the excited states of the system by their total angular momenta $j' = 1/2,3/2,5/2$.

From the known selection rules (when one is interested only in rotational symmetry) [22] one obtains three types of transitions: $j \to j' = j$, which conserves the total momentum, and $j \to j' = j \pm 1$, which change the total momentum by unity. In this case the transitions to the state with total angular momentum $1/2$ are forbidden. The state associated with total momentum $7/2$ does not exist for the Mn^{2+} center. Therefore, we need to consider transition matrix elements only to those excited states, which are described by the total angular momenta $j' = 3/2$ and $j' = 5/2$.

We assume a right-hand circular-polarized electromagnetic wave propagating along the z axis. Then the interaction of the wave with the center is represented by the operator $\hat{\sigma}^+ \propto (x + iy)/\sqrt{2} \propto -Y^1_1(\theta,\varphi)$, where $Y^l_m(\theta,\varphi)$ is the spherical harmonic, which transforms as the component m of the tensor T^l_m of rank l. On the other hand, the interaction with a left-hand circular-polarized wave propagating also along z axis, can be represented as $\hat{\sigma}^- \propto (x - iy)/\sqrt{2} \propto Y^1_{-1}(\theta,\varphi)$.

The symmetry of the matrix elements is given by the Wigner-Eckart theorem [23]. All matrix elements of the same type of transition can be reduced to one matrix element multiplied by corresponding Clebsch-Gordan coefficients

$$V^q_{m'm} = \langle j'm'|T^1_q|jm\rangle = C^{j'm'}_{1qjm}\langle j'||T^1||j\rangle. \qquad (1)$$

Here the index $q = 1$ is for σ^+ polarized light and $q = -1$ is for σ^- light. The term after the Clebsch-Gordan coefficient in (1) does not depend on m, m', and q, thus we will not consider it.

The transition matrix elements can be calculated using the formulas for Clebsch-Gordan coefficients [23]. Circular-polarized light converts pure states with fixed m into pure states with $m' = m \pm 1$. The square of the absolute value of the matrix element is proportional to the probability of the corresponding transition from one pure state to another. The calculated relative intensities of all allowed transitions under right-hand circular-polarized light are shown in Fig. 3. In order to calculate the interaction with the electromagnetic wave, which is linear polarized along one of the axes x or y, one has to form the corresponding linear combinations of the matrix elements for σ^+ and σ^- polarizations.

As one can see in Fig. 3, the occupations of excited states with different projections of the angular momentum on the z axis after circular light pumping are not equal to each other.

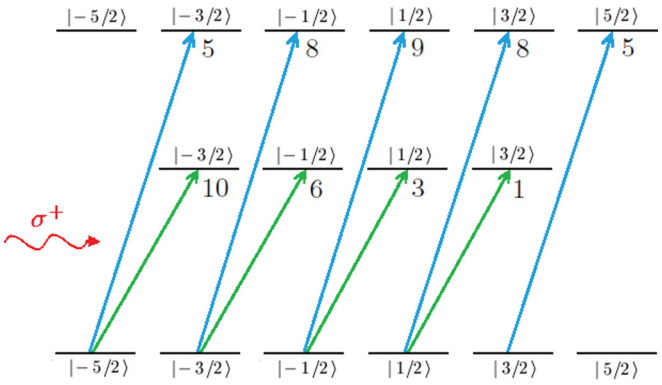

FIG. 3. (Color online) Transitions from ground states to all possible excited states under σ^+ polarized light excitation in electric-dipole approximation. Each arrow corresponds to a transition. The relative intensity of the transition is shown near the arrow.

Therefore circular-polarized light provides a spin orientation of the Mn center. Linear-polarized light does not generate any spin in the system, but it provides different magnitudes of the mean values $\langle j_x'^2\rangle$ and $\langle j_y'^2\rangle$. Thus linear-polarized light distinguishes no directions but axes, which are perpendicular to the direction of light propagation.

We will consider only the recombination processes after pumping and neglect spin relaxation processes because of their very small rates in the experiment. Let the excited states be numbered by the indices n and n', and the ground states by the indices k and k'. Then the density matrix of the system before pumping is given by

$$\rho_{kk'}(0) = \frac{1}{2j+1}\delta_{kk'}, \quad \rho_{nn'}(0) = 0, \quad \rho_{nk}(0) = 0. \qquad (2)$$

A nonzero stationary density matrix arises after pumping in the excited states, and it can be calculated in the regime with a linear dependence on pump intensity as

$$\rho_{nn'} \propto \sum_k V_{nk}^{\lambda} V_{n'k}^{\lambda *}, \qquad (3)$$

where V_{nk}^{λ} is the matrix element of the transition from the ground state k to the excited state n due to interaction of the system with light of λ polarization. The symbol * denotes complex conjugation. Actually, Eq. (3) is a consequence of the Fermi golden rule, which states that the probability of a resonant transition between two quantum-mechanical states is proportional to the square of the matrix elements for interaction with light.

After pumping, spontaneous recombination processes result in luminescence. One can calculate the polarization of the luminescence using the polarization tensor [24]

$$P_{\alpha\beta} = P_0 \sum_{nn'k} \rho_{nn'} V_{nk}^{\alpha *} V_{n'k}^{\beta} = \frac{1}{2}\begin{pmatrix} 1+\xi_3 & \xi_1 - i\xi_2 \\ \xi_1 + i\xi_2 & 1-\xi_3 \end{pmatrix}. \qquad (4)$$

The indices α and β in Eq. (4) denote the x or y axes of polarization. The density matrix $\rho_{nn'}$ obtained from Eq. (3) corresponds to excited states of the system after pumping. $P_0 = 1/(P_{xx} + P_{yy})$ is the normalization constant. The ξ_1, ξ_2, and ξ_3 denote the corresponding Stokes parameters characterizing the luminescence [25]. If $\xi_2 = 1$, then the luminescence shows 100% σ^+ polarization; if $\xi_2 = -1$ −100% σ^- polarization. If $\xi_3 = 1$, then the light is fully linearly polarized along the x axis, and if $\xi_3 = -1$—along the y axis. The ξ_1 parameter describes the linear polarization along the axes rotated around the z axis by $\pi/4$.

TABLE I. Results of calculations.

j'[a]	ρ_c^+ (%)	$\langle j_z'\rangle$[b]	ρ_l^x (%)	$\langle j_x'^2\rangle$[c]
3/2	44.55	−0.75	2.97	1.05
5/2	7.25	0.50	46.38	5.05
Mixed	25.90	−0.125	24.675	3.05

[a]Total angular momentum in an excited state.
[b]Mean value of the angular momentum projection on the z axis for σ^+ pumping.
[c]Mean value of the squared angular momentum projection on the x axis for x-polarized pumping.

Using Eq. (4) one obtains that the luminescence polarization follows the polarization of the pump light, i.e., the PL polarization does not differ from the polarization of the exciting pulse. Circular-polarized light results in circular-polarized luminescence and linear-polarized light results in linear-polarized luminescence along the same axis, which is in good agreement with the experiment. The parameter $\xi_1 = 0$ in all cases. The theoretical values for the parameters $\rho_c = \xi_2$ and $\rho_l = \xi_3$ calculated for the different possible transitions are shown in Table I. The results of these calculations correspond to the maximum values of the PL polarization degrees as the spin relaxation processes are not taken into account in the model.

The experimental values for the luminescence polarizations [shown in Fig. 2(b)] are equal to 8% for circular-polarized pumping and to 10% for linear-polarized pumping. These values can be treated as approximately equal within the experimental accuracy. The comparison shows that the theoretical magnitudes of the corresponding polarization degrees given in the first two rows of Table I are not sufficient for a complete description of the experiment as we consider transitions among pure quantum-mechanical states with fixed total angular momentum.

Hence, we need to examine a combination of transitions to states with different magnitudes of j'. We can roughly estimate PL polarization degrees as mean values of the degrees calculated for pure states. The values obtained by such a procedure are shown in the last row of Table I. They are about 25%, which is still significantly larger than the experimental values. Taking into account that spin relaxation of Mn^{2+} ions in the low energy emitting states is suppressed [see Fig. 2(b)] we conclude that additional depolarization should take place at the initial stage directly after excitation of the Mn^{2+} ions. Indeed, we observe a very fast decay of the linear polarization, while for optical orientation it appears to be too fast to be resolved in time.

At this point, we need to take into account a large Stokes shift (0.2 eV) between the excitation spectrum and the PL spectrum. The loss of orientation/alignment can occur during energy relaxation from the excited state. There are two possible channels for this relaxation: (1) Electron-phonon interaction

that changes the configuration of the d-orbital electrons and manganese ions. This process leads to a modulation of the spin-orbit interaction for the electrons, inducing a spin flip and therefore a depolarization of spin orientation and alignment. Also, it results in a local reduction of the atomic potential energy which provides a lower energy of the reverse optical transitions from the excited state. (2) Excitation energy transfer from one manganese ion to another. In this process spin can also not be preserved due to the fact that the spins of adjacent ions are not parallel to each other. This process can be accompanied by the emission of phonons, so it can also provide a Stokes shift in the PL spectrum. Further identification of the specific mechanism of spin loss during the energy relaxation will require more detailed investigations in the future.

IV. CONCLUSION

We have found resonant optical orientation and alignment of Mn^{2+} ion spins in the diluted magnetic semiconductor (Cd,Mn)Te. These phenomena are manifested by circular- and linear-polarized emission of the Mn^{2+} centers at low temperatures when the spin relaxation of the Mn^{2+} ions is strongly suppressed. The spin relaxation time is in the order of 1 ms, which is much longer than the recombination time of the Mn^{2+} excited state equal to about 23 μs. A phenomenological theory has been developed, based on the approximation of isolated centers. We have demonstrated that the experimental data do not contradict the theoretical limits for the allowed intracenter optical transitions that provide a maximum possible polarization of the luminescence of about 25%. Possible mechanisms of spin depolarization leading to a reduction of intracenter photoluminescence polarization have been discussed. Our results have revealed an optically addressable center offering perspectives for optical control and recording of information in the spin glass phase which is especially interesting for memory devices and image recognition.

ACKNOWLEDGMENTS

We acknowledge the support of this work by the Russian Science Foundation (Project No. 14-42-00015), the Deutsche Forschungsgemeinschaft via ICRC TRR 160, and by the Bundesministerium für Bildung und Forschung (Project No. 05K12PE1). V.L.K. acknowledges support of the Deutsche Forschungsgemeinschaft within the Gerhard Mercator professorship program.

[1] J. R. Weber, W. F. Koehl, J. B. Varley, A. Janotti, B. B. Buckley, C. G. Van de Walle, and D. D. Awschalom, Proc. Natl. Acad. Sci. USA **107**, 8513 (2010).
[2] F. Jelezko and J. Wrachtrup, Phys. Status Solidi A **203**, 3207 (2006).
[3] A. Gruber, A. Dräbenstedt, C. Tietz, L. Fleury, J. Wrachtrup, and C. Borczyskowski, Science **276**, 2012 (1997).
[4] P. G. Baranov, A. P. Bundakova, A. A. Soltamova, S. B. Orlinskii, I. V. Borovykh, R. Zondervan, R. Verberk, and J. Schmidt, Phys. Rev. B **83**, 125203 (2011).
[5] W. F. Koehl, B. B. Buckley, F. J. Heremans, G. Calusine, and D. D. Awschalom, Nature (London) **479**, 84 (2011).
[6] H. Kraus, V. A. Soltamov, D. Riedel, S. Väth, F. Fuchs, A. Sperlich, P. G. Baranov, V. Dyakonov, and G. V. Astakhov, Nat. Phys. **10**, 157 (2014).
[7] M. Widmann, S.-Y. Lee, T. Rendler, N. T. Son, H. Fedder, S. Paik, L.-P. Yang, N. Zhao, S. Yang, I. Booker *et al.*, Nat. Mater. **14**, 164 (2015).
[8] J. M. Taylor, P. Cappellaro, L. Childress, L. Jiang, D. Budker, P. R. Hemmer, A. Yacoby, R. Walsworth, and M. D. Lukin, Nat. Phys. **4**, 810 (2008).
[9] D. Rugar, H. J. Mamin, M. H. Sherwood, M. Kim, C. T. Rettner, K. Ohno, and D. D. Awschalom, Nat. Nanotechnol. **10**, 120 (2015).
[10] J. K. Furdyna, J. Appl. Phys. **64**, R29 (1988).
[11] V. F. Agekyan, Phys. Solid State **44**, 2013 (2002).
[12] *Introduction to the Physics of Diluted Magnetic Semiconductors*, edited by J. A. Gaj and J. Kossut (Springer-Verlag, Berlin, Heidelberg, 2011).
[13] V. G. Abramishvili, A. V. Komarov, S. M. Ryabchenko, and Y. G. Semenov, Solid State Commun. **78**, 1069 (1991).
[14] M. Nawrocki, Y. G. Rubo, J. P. Lascaray, and D. Coquillat, Phys. Rev. B **52**, R2241 (1995).
[15] E. Müller, W. Gebhardt, and V. Gerhardt, Phys. Status Solidi B **113**, 209 (1982).
[16] H. Schenk, M. Wolf, G. Mackh, U. Zehnder, W. Ossau, A. Waag, and G. Landwehr, J. Appl. Phys. **79**, 8704 (1996).
[17] C. Le Gall, L. Besombes, H. Boukari, R. Kolodka, J. Cibert, and H. Mariette, Phys. Rev. Lett. **102**, 127402 (2009).
[18] M. Goryca, T. Kazimierczuk, M. Nawrocki, A. Golnik, J. A. Gaj, P. Kossacki, P. Wojnar, and G. Karczewski, Phys. Rev. Lett. **103**, 087401 (2009).
[19] D. Heiman, P. Becla, R. Kershaw, D. Ridgley, K. Dwight, A. Wold, and R. R. Galazka, Phys. Rev. B **34**, 3961 (1986).
[20] M. M. Moriwaki, W. M. Becker, W. Gebhardt, and R. R. Galazka, Phys. Rev. B **26**, 3165 (1982).
[21] N. Vasilyev, J. Lumin. **132**, 1215 (2012).
[22] L. D. Landau and E. M. Lifshitz, *Quantum Mechanics: Non-Relativistic Theory*, Course of Theoretical Physics Vol. 3 (Pergamon Press, Oxford, 1977).
[23] D. Varshalovich, A. Moskalev, and V. Khersonskii, *Quantum Theory of Angular Momentum* (World Scientific, Singapore, 1989).
[24] E. L. Ivchenko and G. E. Pikus, *Superlattices and Other Heterostructures*, Solid State Sciences Vol. 110 (Springer-Verlag, Berlin, Heidelberg, 1995).
[25] L. D. Landau and E. M. Lifshitz, *The Classical Theory of Fields*, Course of Theoretical Physics Vol. 2 (Pergamon Press, Oxford, 1971).